Microwave Scattering and Noise Emission from Afterglow Plasmas in a Magnetic Field

F. A. Blum,* L. O. Bauer,† R. W. Gould, and R. L. Stenzel
California Institute of Technology, Pasadena, California
(Received 15 November 1968)

The microwave reflection and noise emission (extraordinary mode) from cylindrical rare-gas (He, Ne, Ar) afterglow plasmas in an axial magnetic field is described. Reflection and noise emission are measured as a function of magnetic field near electron cyclotron resonance ($\omega \approx \omega_c$) with electron density as a parameter ($\omega_p < \omega$). A broad peak, which shifts to lower values of ω_c/ω as electron density increases, is observed for $(\omega_c/\omega) \leq 1$. For all values of electron density a second sharp peak is found very close to cyclotron resonance in reflection measurements. This peak does not occur in the emission data. Calculations of reflection and emission using a theoretical model consisting of a one-dimensional, cold plasma slab with nonuniform electron density yield results in qualitative agreement with the observations. Both the experimental and theoretical results suggest that the broad, density-dependent peak involves resonance effects at the upper hybrid frequency ($\omega_h^2 = \omega_c^2 + \omega_p^2$) of the plasma.

I. INTRODUCTION

The microwave properties of bounded hot plasmas in a magnetic field have received considerable attention in the past few years. Intense noise radiation at harmonics of the electron cyclotron frequency,[1] the subsidiary resonances near the second (and sometimes the higher) harmonic of the cyclotron frequency,[2] and a variety of other experiments[3] support the theory of dispersion of waves in a hot magnetoplasma put forth by Bernstein.[4] These experiments and the related theoretical developments have greatly increased the understanding of hot-plasma effects in a magnetic field, where finite Larmor radius effects are important.

The microwave properties of plasmas with low electron temperature (and low electron density) have received much less attention. Noise emission[5] and echoes[6] have been studied in cesium plasmas and some studies of microwave effects in rare-gas afterglow plasmas have been made.[7-11] In particular, the latter have been used primarily in studies of the cyclotron resonance echo.[8-10] It was in connection with our own study of echoes[10] that the present study of scattering and emission near cyclotron resonance was begun.

Under conditions of low electron temperature and density, cyclotron harmonic effects are no longer significant. At sufficiently low densities one expects simple, single-particle, cyclotron resonance effects near $\omega_c = \omega$ where ω_c is the electron cyclotron frequency and ω is the signal frequency. At higher densities, plasma wave theory[12] predicts wave dispersion with cutoffs and resonances which depend upon the polarization and direction of propagation, as well as the plasma parameters. Because of our experimental geometry (described later) we are concerned with the extraordinary mode which propagates and is elliptically polarized in a plane perpendicular to the static magnetic field. In a uniform unbounded plasma this mode has a resonance at the upper hybrid frequency $\omega_h^2 = \omega_c^2 + \omega_p^2$ where ω_p is the electron plasma frequency. Upper hybrid resonance effects in inhomogeneous laboratory plasmas have been previously reported.[5,11,13] Our experiments are similar in concept to those of Kuckes and Wong[5] and Tetenbaum and Bailey[7], except that our plasma column is small compared with a waveguide wavelength ($2\pi/\lambda_g = 0.4$) (where a is the

* Present address: Lincoln Laboratory, Massachusetts Institute of Technology, Lexington, Massachusetts.
† Present address: Applied Solid State Research Department, Hughes Research Laboratories, Newport Beach, California.
[1] G. Landauer, J. Nucl. Energy, Pt. C **4**, 395 (1962).
[2] S. J. Buchsbaum and A. Hasegawa, Phys. Rev. **143**, 303 (1966).
[3] For a review of these phenomena, see F. W. Crawford, Nucl. Fusion **5**, 73 (1965).
[4] I. B. Bernstein, Phys. Rev. **109**, 10 (1958).
[5] A. F. Kuckes and A. Y. Wong, Phys. Rev. Letters **13**, 306 (1964); Phys. Fluids **8**, 1161 (1965).
[6] D. E. Kaplan, R. M. Hill, and A. Y. Wong, Phys. Letters **22**, 585 (1965).
[7] S. J. Tetenbaum and H. N. Bailey, Phys. Rev. Letters **19**, 12 (1967).
[8] R. M. Hill and D. E. Kaplan, Phys. Rev. Letters **14**, 1062 (1965); G. F. Herrmann, R. M. Hill, and D. E. Kaplan, Phys. Rev. **156**, 118 (1967).
[9] R. W. Harp, R. L. Bruce, and F. W. Crawford, J. Appl. Phys. **38**, 3385 (1967).
[10] L. O. Bauer, F. A. Blum, and R. W. Gould, Phys. Rev. Letters **20**, 435 (1968).
[11] R. M. Hill, D. E. Kaplan, and S. K. Ichiki, Phys. Rev. Letters **19**, 154 (1967).
[12] T. H. Stix, *The Theory of Plasma Waves* (McGraw-Hill Book Company, New York, 1962), Chap. 2.
[13] G. Bekefi, J. D. Coccoli, E. B. Hooper, and S. J. Buchsbaum, Phys. Rev. Letters **9**, 6 (1962); K. Mitani, H. Kubo, and S. Tanaka, J. Phys. Soc. Japan **19**, 211 (1964).

column radius). Our results show evidence of both the upper hybrid resonance and cyclotron resonance.

Section II of this paper describes measurements of the continuous wave (cw) reflection as a function of magnetic field near electron cyclotron resonance with electron density as a parameter. Section III describes the noise emission under similar conditions. The scattering and the emission data show similar features, both having a broad upper hybrid resonance in the region $(\omega_c/\omega) \leq 1$. However, the reflection data show an additional narrow peak at cyclotron resonance. Section IV gives some theoretical calculations using a cold inhomogeneous plasma slab model. Reflection and emission calculated by incorporating this plasma slab into an appropriate transmission line circuit are in qualitative agreement with the theory.

II. REFLECTION MEASUREMENTS

The plasmas studied experimentally were rare-gas (He, Ne, Ar) afterglow discharges created by a 21-MHz rf pulse of about 50 μsec in length. They were contained in a glass cylinder of 1.8 cm i.d. and about 1 m in length, aligned coaxially with a static magnetic field $\mathbf{B}_0$ of a solenoid formed by 10 pancake-type coils. The glass tube was inserted through and perpendicular to the narrow walls of a waveguide section (S and X bands) so that the configuration for the microwaves was $\mathbf{E} \perp \mathbf{k} \perp \mathbf{B}_0$ where $\mathbf{E}$ is the unperturbed electric field and $\mathbf{k}$ is the propagation vector of the signal. The magnetic field $\mathbf{B}_0$ was homogeneous to one part in 10^4 over the volume of plasma within the waveguide.

In order to keep impurity concentrations at a minimum, the plasma vessel was baked at 400°C overnight and evacuated, achieving an empty vessel pressure of 10^{-7} mm Hg. The gases used were Matheson Company research grade (minimum purity by volume: Ar and He, 99.9995%; Ne, 99.995%) and were introduced to the system by a controlled leak valve at pressures typically a few tens of microns. Neutral gas pressures given are accurate to about $\pm 5\%$.

The plasma was placed in one of the side arms of a balanced microwave bridge system formed by the use of a magic tee (see Fig. 1). Both side arms were terminated in matched loads. A magic tee has the property[14] that if the H-arm (input) and E-arm (output) are terminated in matched loads and a signal E_{in} enters the input, the signal in the output arm E_{out} is given by

$$E_{out} = (\Gamma_1 - \Gamma_2)\tfrac{1}{2}E_{in}, \tag{1}$$

where Γ_1 and Γ_2 are the complex reflection coefficients seen at the junction looking into side arms one and two, respectively. If we assume that the scattering from the waveguide holes and the glass are such that the scattered fields superpose, Γ_1 is the sum of the reflection coefficient from the plasma Γ_p and from the glass and holes Γ_g. Equation (1) becomes

$$E_{out} = (\Gamma_p + \Gamma_g - \Gamma_2)\tfrac{1}{2}E_{in}.$$

A slide screw turner placed in arm 2 and adjusted to cancel reflections (in the absence of the plasma) from the glass tube and holes, giving $\Gamma_2 = \Gamma_g$ yields $E_{out} = \Gamma_p \tfrac{1}{2}E_{in}$. Thus a properly balanced microwave bridge apparatus yields the reflection coefficient of the plasma directly, eliminating the unwanted reflections due to undesirable experimental conditions such as holes in the waveguide walls. For the magic tees and frequencies used, the maximum voltage standing wave ratio measured when looking into any individual arm with the other three terminated was about 1.1 for both S band and X band. Therefore, any errors in the measured reflection coefficients should be less than a few percent.

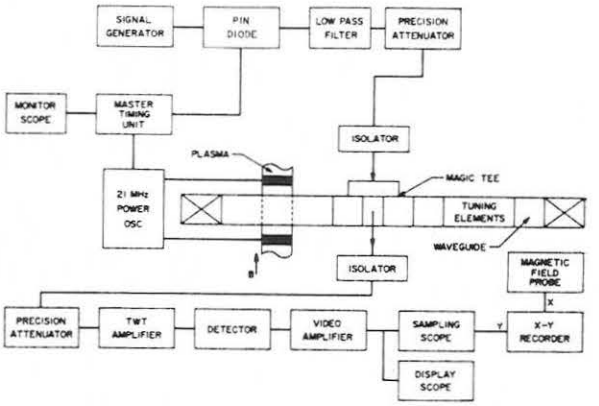

FIG. 1. Block diagram of the experimental apparatus.

Figure 1 gives a block diagram of the instrumentation and shows the experimental geometry. The 21-MHz, 100 W power oscillator is pulsed creating a plasma and turning off at time $t = 0$ (by definition). The oscillator is capacitively coupled to the plasma by means of a tuned, parallel $L\,C$ circuit, where part of the capacitance is furnished by two copper sleeves (10 cm long) tightly fitted on the glass tube and placed on opposite sides of the waveguide. The microwave signal generator produces a continuous wave signal which is pulse modulated (about 1 μsec

[14] L. B. Young in *Techniques of Microwave Measurements*, C. G. Montgomery, Ed. (McGraw-Hill Book Company, New York, 1948), Chap. 9, p. 515.

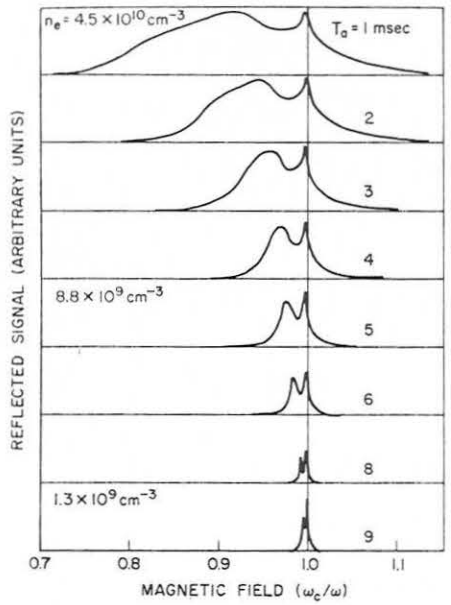

FIG. 2. Reflection vs magnetic field for a neon afterglow at 47μ Hg with -30 dB incident power (S band).

width) by the PIN diode switch at the time $t = T_a$ (afterglow time). The master timing circuits repeat this sequence at 60 Hz. The plasma density decays with a time constant of typically between a few hundred microseconds and a few milliseconds, depending on the gas and the conditions. Thus, a reflection experiment using pulses short compared with the decay time is performed at constant plasma density for all practical purposes. Although such pulses are not cw, experiments using them yield results essentially identical to a cw measurement if the spectral width ($\approx$1 MHz) of the pulse is narrow compared with the spectrum width of the plasma response. Also, the pulsed incident signal helps minimize electron heating by the microwaves. Following reflection from the plasma, the signal is amplified, crystal detected, and sampled at a fixed time using a sampling oscilloscope. The voltage drop across a resistor in series with the magnet coils is directly proportional to the magnetic field strength and was calibrated using standard NMR techniques. Continuous plots on an X–Y recorder of the reflection from the plasma as a function of magnetic field and electron density are thus facilitated. Instrument noise in the reflection data is on the order of the width of the traces shown.

The electron temperature of afterglow plasmas such as those studied here is thought to decay very rapidly,[8] with time constants as short as tens of microseconds. Electron–neutral collisions cannot account for such fast energy relaxation and not much is understood about the actual processes. Little quantitative evidence is available. However, preliminary experiments in our laboratory show radiation temperatures typically down to $\lesssim 500$°K at $T = 1$ msec for neon and argon. Therefore, it will be assumed that the electron temperature is constant and low (at most a few thousand degrees) for all data taken in the late afterglow, yielding a direct relation between T_a and electron density.

Basically, we would like to study the spectral response of the plasma by measuring the reflection from it as a function of frequency. However, experimentally it is convenient to hold ω fixed and vary the magnetic field, while sampling at a fixed electron density. This procedure is theoretically entirely equivalent to frequency variation since only the ratios (ω_c/ω) and (ω_p/ω) are relevant. As a practical matter, we implicitly assume that the plasma conditions (peak density, density profile, decay time, etc.) do not change with magnetic field. The values of (ω_c/ω) shown in the data are accurate to within $\pm 0.2\%$.

Although not the subject of this paper, reflection experiments performed at early afterglow times, where the electron temperature is still relatively high ($\sim$1 eV), give a perspective on the type of plasmas we are studying. Two classical hot-plasma effects were found[15]: (1) cyclotron harmonic resonances[3] near $(\omega_c/\omega) = 1/n$, $n = 2, 3 \cdots$, and (2) the Buchsbaum–Hasegawa modes,[2] just above $(\omega_c/\omega) = 0.5$. The cyclotron harmonic effects disappear virtually as soon as the experiment is performed in the afterglow rather than in the active discharge. The evidence of the Buchsbaum–Hasegawa modes also disappears quickly (for $T_a \gtrsim 100$ μsec). Here we have another indication that the electron temperature decays very rapidly.

Figures 2 and 3(a) show the reflection from neon and argon afterglows at later T_a where the temperature is low. These data were taken in the S-band apparatus ($\omega/2\pi = 3.0$ GHz) and show clearly the presence of collective behavior. As is the case for all data in this paper, the receiver gain is the same for all curves in a given figure unless otherwise stated. The light horizontal lines locate the zero reflection reference lines. The sharp peak in reflection near cyclotron resonance $(\omega_c/\omega) = 1$, and the broad peak at lower values of (ω_c/ω) are very characteristic for both neon and argon. Note the consistent scaling of the general features of the data with T_a and, therefore, electron density, since we

[15] F. A. Blum, Ph. D. thesis, California Institute of Technology (1968).

assume that the electron temperature has already reached a constant level. The peak in the scattering which significantly shifts and broadens at high electron densities has the general appearance of a common feature of reflection, emission, and absorption spectra of cyclotron-resonance experiments reported by other observers.[2,16,17] This feature is attributed to the upper hybrid resonance of a cold, inhomogeneous plasma.[18] Note that a collision broadening estimate of the width of this resonance is off by an order of magnitude. However, since small laboratory plasmas of the type used here are rather inhomogeneous, the plasma possesses a range of upper hybrid frequencies $\omega_h^2 = \omega_c^2 + \omega_p^2$. This nonuniform density broadening is responsible for the width of the upper hybrid resonance. Significant scattering apparently only takes place for $1 \gtrsim (\omega_c/\omega) \gtrsim (\omega_c/\omega_{h0})$ where $\omega_{h0}^2 = \omega_c^2 + \omega_{p0}^2$ is the maximum upper hybrid frequency and ω_{p0} is the maximum local plasma frequency. In fact, the onset of significant scattering at low values of (ω_c/ω) has proved to be a good measure of the maximum electron density of nonuniform plasma columns.[17] The onset point on the (ω_c/ω) axis is taken to be such that the incident signal frequency is equal to the maximum upper hybrid frequency, i.e., $\omega = \omega_{h0}$. This interpretation is the source of the electron density estimates given in Figs. 2 and 3(a), and is consistent with the interpretation of two-pulse echo experiments performed on the same plasmas.[10] The definition of the onset point is somewhat arbitrary. Some curves show a slight break in the slope on the rising side (as ω_c/ω is increased) of the broad peak. This break may mark the location of (ω_c/ω_{h0}). It is sometimes more pronounced than shown in Figs. 2 and 3(a), but is not easily followed as T_a increases. As a matter of consistency, the onset point is taken to be that value of (ω_c/ω) such that the reflection is 20% of its peak value.

Reflection curves for helium are given in Fig. 3(b). Although the results scale consistently with electron density, the data are markedly different from that for neon and argon. The narrow reflection peak at cyclotron resonance is still present. However, the pronounced upper hybrid peak has been replaced by a sharp break in the slope of the curves. Lacking a quantitative theory, we have associated this break with (ω/ω_{h0}) in arriving at the electron densities given.

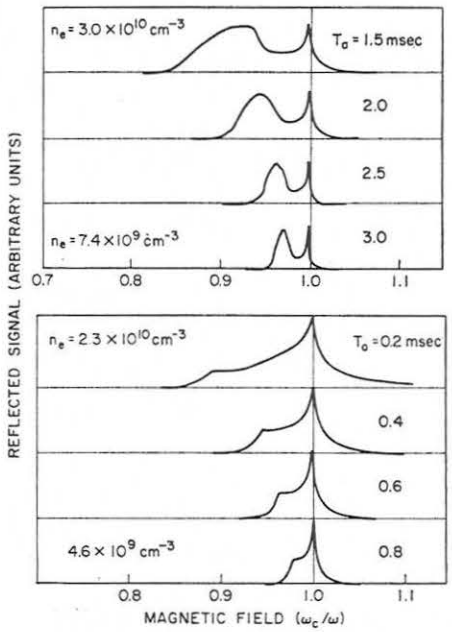

FIG. 3(a) (Top) Reflection vs magnetic field for an argon afterglow at 39μ Hg with -23 dB incident power (S band). (b) (Bottom) Reflection vs magnetic field for a helium afterglow at 12μ Hg with -23 dB incident power (S band).

The narrow cyclotron resonance peak is an anomaly with respect to previous cold-plasma interpretation. Observations[16] in other plasmas in which the electron temperature is higher do not show such a cyclotron resonance effect. We also find that the cyclotron resonance peak tends to disappear at high temperatures.[15] The relevance of these effects to appropriate theoretical models will be discussed below. Although detailed studies of the reflection as a function of neutral gas pressure were not made, the data are qualitatively similar for pressures as high as 500 μ Hg. Also, the power reflection is typically about 10% at the peaks of the curves for n_e about 10^{10} cm^{-3} in the afterglow, and about 50% at the peak in the active discharge. Note that the peak reflection coefficients are an extremely slow function of electron density.

Figure 4 displays the electron density vs T_a as taken from the data of Figs. 2 and 3. The data points for each gas fitted fairly well by a simple exponential decay. The rapid decay of the helium afterglow is probably related to the fact that its low-energy electron–neutral collision frequency is much higher than that of argon and neon.[19] The

[16] G. Bekefi, J. D. Coccoli, E. B. Hooper, and S. J. Buchsbaum, Phys. Rev. Letters 9, 6 (1962); S. Tanaka, H. Kubo, and K. Mitani, J. Phys. Soc. Japan 20, 462 (1965).

[17] H. J. Schmitt, G. Meltz, and P. J. Freyheit, Phys. Rev. 139, A1432 (1965); C. D. Lustig, *ibid.* 139, A63 (1965); S. Tanaka, J. Phys. Soc. Japan 21, 1804 (1966).

[18] S. J. Buchsbaum, Bull. Am. Phys. Soc. 7, 151 (1962); S. J. Buchsbaum, L. Mower, and S. C. Brown, Phys. Fluids 3, 806 (1960).

[19] S. C. Brown, *Basic Data of Plasma Physics* (M. I. T. Press, Cambridge, Massachusetts, 1967), Chap. 1.

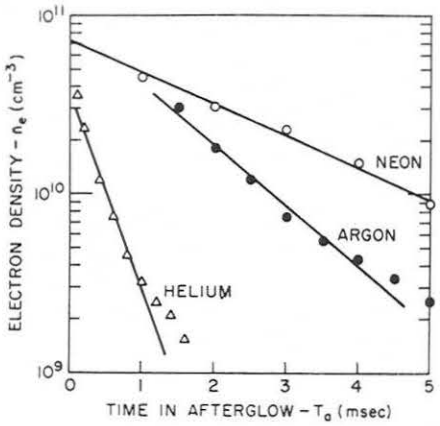

FIG. 4. Electron density vs time in the afterglow for Ne, Ar, and He as deduced from the cw reflection data of Figs. 2 and 3.

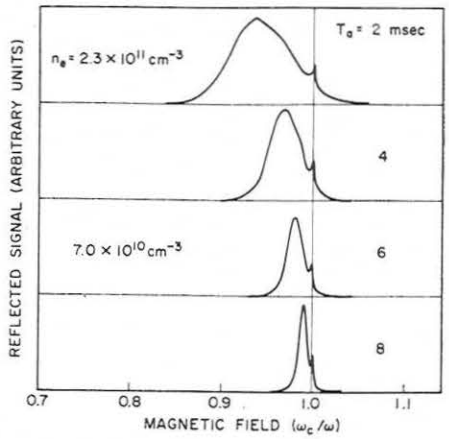

FIG. 5. Reflection vs magnetic field for an argon afterglow at 37μ Hg with a −21 dB signal (X band).

usefulness of the reflection measurements as a density diagnostic technique is immediately apparent. A quantitative theory might facilitate relatively accurate measurements for densities greater than about 10^9 cm^{-3}.

Reflection measurements were also performed at X-band frequencies, checking the generality of the above results. Some typical results are shown in Fig. 5. The basic components used at X band ($\omega/2\pi$ = 9.0 GHz) were functionally the same as those used at S band. However, a section of tapered transition to increased height waveguide (0.9 × 0.9 in.) was used to accommodate the glass tube (same diameter as used before). The general features are quite similar to the S-band data. However, the peak at cyclotron resonance is now diminished relative to the upper hybrid peak. The electron densities were estimated using the same interpretation of the results given for the S-band data.

III. NOISE EMISSION MEASUREMENTS

A time-gated microwave radiometer was used to measure the thermal noise emission from the plasmas as a function of magnetic field and electron density. Basically, the radiometer is a superheterodyne microwave receiver which is turned on for an interval of 1 μsec at the time T_a in the afterglow. The local oscillator frequency is 3.0 GHz. The i.f. has a center frequency of 7 MHz and a half-power bandwidth of 8 MHz. The image was not filtered and presents no problem as long as the characteristic spectral widths of the plasma emission are greater than about 25 MHz, which is the case for all data shown. The receiver was gated at the last i.f. stage. The resulting pulses were synchronously detected at the frequency of repetition of the experiment, with a time constant of 1 sec. The output of the synchronous detector was used to drive an X–Y recorder. The noise figure of the microwave receiver is about 5 dB. The plasma was again placed in an S-band waveguide in such a manner that the configuration $\mathbf{E} \perp \mathbf{k} \perp \mathbf{B}_0$ was maintained. An isolator was placed between the plasma and the receiver, and a termination was placed behind the plasma (a bridge system was not employed). Other experimental conditions were the same as those of the reflection experiments.

The relative noise emission from an argon afterglow similar to that used in obtaining the reflection data of Fig. 3(a) is given in Fig. 6. The magnetic field was varied while the local oscillator frequency was held fixed. The light horizontal lines approximately located the output level for no plasma emission. Note the relationship of this data to the reflection data. The emission shows the upper hybrid peak, but lacks a cyclotron resonance peak. However, there is a distinct break in the slope of the curves at cyclotron resonance. Figure 7 gives the noise emission data for a helium afterglow. The plasma conditions are essentially the same as those used in obtaining the reflection data of Fig. 3(b). The qualitative similarity between the helium reflection and the emission data is apparent.

Considerable care must be exercised in taking emission data of the type shown here. A high level of isolation ($\approx$50 dB) between the plasma and the local oscillator of the receiver is required. Apparently, a relatively weak microwave signal ($\approx$10 μW) incident on the plasma is sufficient to significantly enhance the radiation at frequencies 10 MHz removed from that microwave signal when $\omega \approx \omega_c$, yielding a spurious cyclotron resonance peak.

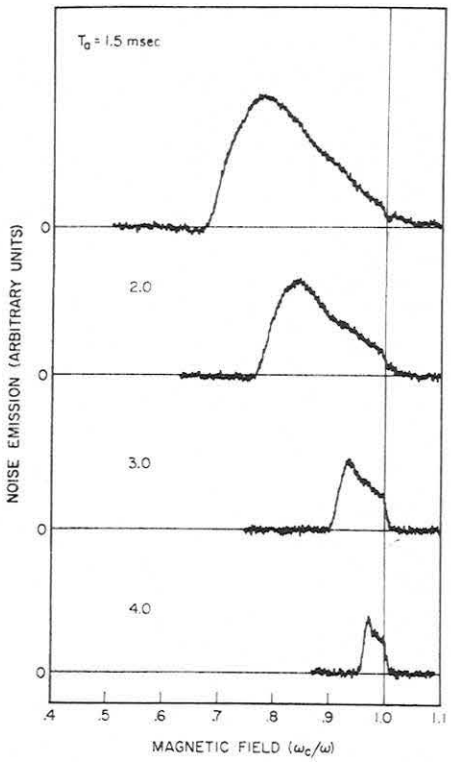

FIG. 6. Noise emission vs magnetic field for an argon afterglow (neutral pressure: 21μ Hg).

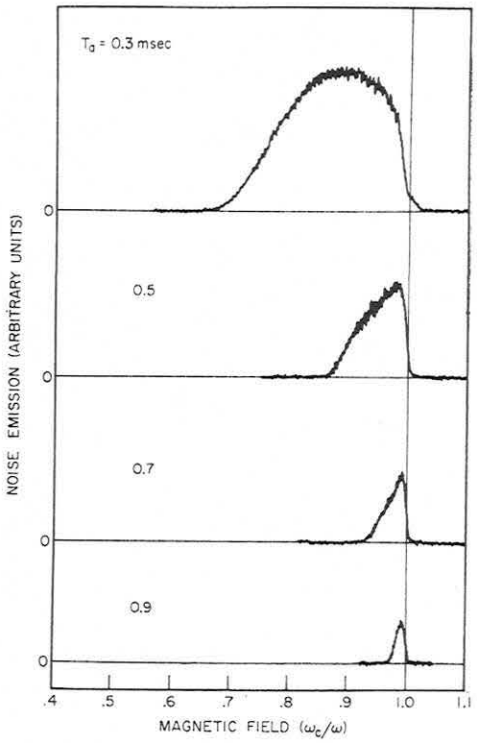

FIG. 7. Noise emission vs magnetic field for a helium afterglow (neutral pressure: 20μ Hg).

Earlier measurements[15] with low isolation ($\approx$20 dB) suffered from this difficulty.

IV. COLD NONUNIFORM PLASMA THEORY

Attempting to account qualitatively for the reflection and emission data, we consider a one-dimensional inhomogeneous cold plasma slab of thickness $2a$ situated in a uniform magnetic field B which is parallel to the slab faces [see Fig. 8(a)]. For convenience, the steady-state electron density is assumed to depend on x in such a manner that $\omega_p^2(x) = \omega_{p0}^2 (1 - x^2/a^2)$. Collisions are neglected. We consider the plasma to be charge neutralized in the steady state by a background of fixed, positive ions. Simulating the conditions of the experiment, we place a short section of this plasma slab in a parallel-plate transmission line which has a matched generator at one end and is terminated in its characteristic impedance Z_0 at the other end as shown in Fig. 8(a). In order to do this we must take the plasma to be bounded in the plane perpendicular to the x direction, in effect, removing the restriction to a one-dimensional problem. However, we will assume that the plasma dimensions are such that the properties of the one-dimensional slab are a good approximation, neglecting fringing field effects. Since in the experiment the lateral dimensions of the plasma are small compared with the guide wavelength, we replace the plasma of Fig. 8(a) which is distributed along the transmission line by a simple lumped-element equivalent circuit as shown in Fig. 8(b). The circuit element C_1 is the capacitance of the vacuum between the plasma and the conducting

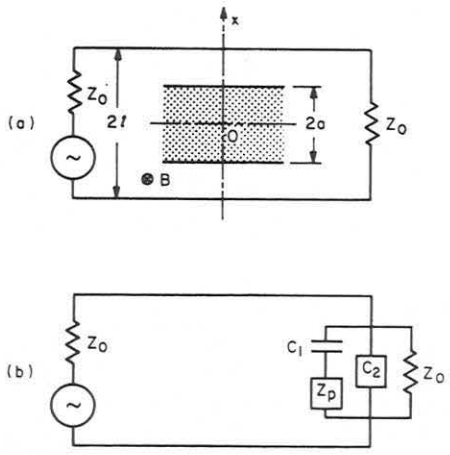

FIG. 8(a) Diagram showing geometry of the plasma-slab and parallel-plate transmission line which comprise the theoretical model. (b) Lumped-element equivalent circuit of the plasma-slab, transmission-line model.

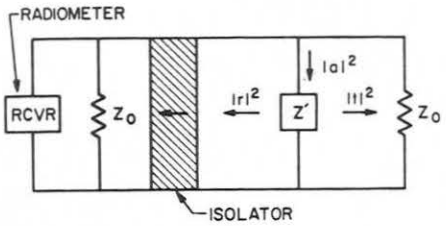

FIG. 9. Schematic diagram of transmission line equivalent of noise emission experimental apparatus. Z' is the total impedance of the plasma and the capacitors C_1 and C_2 of Fig. 8.

plates, and is given by $C_1 = \epsilon_0 A/2(l - a)$, where ϵ_0 is the permittivity of free space and A is the lateral area of the capacitor–slab system. The negative capacitance C_2 results from the equivalent circuit approximation and is equal to $-(\epsilon_0 A/2l)$.

The dependence on (ω_c/ω) of the reflection coefficient seen at the generator on the transmission line will yield the theoretical equivalent of the experimental reflection data. Removing the ideal generator from the circuit, and placing an isolator between the impedance Z_0 and the plasma, yields the configurations of the noise emission experiments (see Fig. 9). Use of the Nyquist theorem will permit one to compute the emission vs (ω_c/ω). In either case one needs the expression for the plasma impedance which we will now derive.

We restrict our attention to electrostatic oscillations of the plasma so that we retain only Poisson's equation of Maxwell's equations. For such one-dimensional electrostatic systems the total current density (particle or fluid current plus displacement current) $J_0(t)$ in the x direction is a spatial invariant. For a system of particles which can be described by a local relation between particle currents and the electric field, one can derive an equivalent permittivity so that $J_0 = i\omega\epsilon E$, where ω is the oscillation frequency and E is the electric field. For a cold uniform collisionless plasma[20]

$$\left(\frac{\epsilon}{\epsilon_0}\right) = 1 - \frac{\omega_p^2}{\omega^2 - \omega_c^2}. \tag{2}$$

For an inhomogeneous cold plasma ϵ is a function of x and Eq. (2) is valid locally. The plasma impedance is then given by

$$\begin{aligned} Z_p &= -\frac{1}{A}\int_{-a}^{a}\frac{E}{J_0}\,dx \\ &= \frac{(\omega_c^2 - \omega^2)}{i\omega\epsilon_0 A}\int_{-a}^{a}\frac{dx}{\omega_c^2 + \omega_p^2(x) - \omega^2}. \end{aligned} \tag{3}$$

[20] W. P. Allis, S. J. Buchsbaum, and A. Bers, *Waves in Anisotropic Plasmas* (M. I. T. Press, Cambridge, Massachusetts, 1963), Chap. 2, p. 23.

As the integrand in Eq. (3) stands it has simple poles at symmetrical values of x when ω lies in the band of upper hybrid frequencies $\omega_c \leq \omega \leq \omega_{h0}$. Inclusion of collision effects removes this singularity from the path of integration. However, one can evaluate the integral in the limit of zero collision frequency using the Dirac formulation of such integrals. These steps are carried out in the Appendix, giving an exact closed form expression for Z_p over the entire real frequency domain. The impedance is found to have a real part only when ω is in the range of upper hybrid frequencies. The fact that there is a real part to the impedance in the absence of collisional processes is a property of the continuum nature of the normal modes of the cold inhomogeneous plasma. Basically, the plasma resonates with any applied field whose frequency ω is such that[21] $\omega^2 = \omega_h^2(x)$. The resonance is local and occurs at those points x where $\omega^2 = \omega_h^2(x)$, i.e., the condition of local upper hybrid resonance. In our collisionless model the electric field is infinite at the resonance points. However, this singularity in the normal mode field is integrable in the Dirac sense and one obtains a finite slab impedance. Of course, in a real plasma the strength of the electric field at the resonance points is limited by the dissipation processes (collisions). Thus, the expression for Z_p given in the Appendix is the limiting case and is approximately valid for $(\nu/\omega) \ll 1$, where ν is collision frequency of electrons with other plasma species. In our experiments, $(\nu/\omega) \approx 10^{-2}$–$10^{-3}$.

The complex reflection coefficient measured at the generator of Fig. 8(b) is given by

$$r = -Z_0/(2Z' + Z_0),$$

where Z' is the combination impedance of the plasma, the capacitance C_1, and the negative capacitance C_2,

$$\frac{1}{Z'} = -\frac{i\omega\epsilon_0 A}{2l} + \frac{1}{Z_p + [2(l - a)/i\omega\epsilon_0 A]}. \tag{4}$$

Experimentally, a square-law detector would measure $|r|^2$ which is a function of the four variables: $R \equiv (Z_0\omega\epsilon_0 A/2l)$, (l/a), (ω_{p0}/ω), and (ω_c/ω).

In Fig. 10 we plot $|r|^2$ vs (ω_c/ω) for several values of $(\omega_{p0}/\omega)^2$. The values of $(\omega_{p0}/\omega)^2$ were chosen comparable to those found in the experiments. The parameters R and (l/a) do not have exact experimental equivalents. We have taken $R = 5$ and

[21] For a discussion of this phenomenon for a plasma in the absence of a magnetic field, see: E. M. Barston, Ann. Phys. (N. Y.) **29**, 282 (1964); see also, R. W. Gould and F. A. Blum, *Eighth International Conference on Phenomena in Ionized Gazes* (Springer-Verlag, Vienna 1967), p. 405.

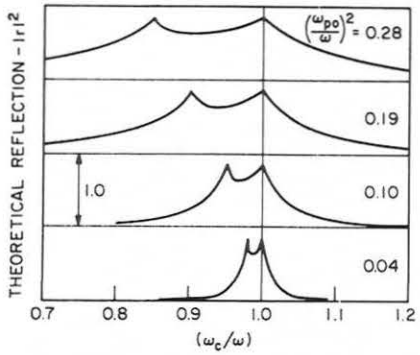

FIG. 10. Theoretical reflection ($|r|^2$) vs magnetic field with electron density as a parameter.

$(l/a) = 2$ as reasonable estimates. The parameter R determines the relative size of the characteristic line impedance Z_0 and the plasma impedance Z_p. Roughly, R sets the over-all scale of the amount of reflection, while (l/a) controls the relative height of the two peaks. The resemblance between the neon and argon experimental reflection curves and the theoretical ones is apparent. One peak in the theoretical reflection occurs at cyclotron resonance, while a second peak occurs at the maximum upper hybrid frequency of the slab. The two peaks occur because $|Z_p/Z_0|$ is very high near $\omega = \omega_{h0}$ and very low near $\omega = \omega_c$. Either condition yields a high reflection coefficient. The height of the two peaks is the same and is independent of electron density. The experimental peaks are also approximately equal and decrease very slowly with decreasing electron density. The calculated peak values of $|r|^2$ are somewhat higher than those observed experimentally. Reduction in R would lower these values and change the shape of the curves somewhat. However, no new qualitative features appear and the two characteristic peaks are always present. The quantitative difference between theory and experiment on the exact position of the upper hybrid peak is one shortcoming of the adopted model. Helium represents an anomaly with respect to the other gases and the calculated curves. However, it is possible to produce theoretical curves somewhat similar to the helium by adjusting R and (l/a).

Assuming thermodynamic equilibrium exists in the electron gas and in the waveguide components, and the radiation field in the waveguide, Nyquist's theorem[22] can be used to calculate the noise emission of the plasma. The total noise power per unit bandwidth P_N passing from the isolator to the radiometer in Fig. 9 is

$$P_N = \kappa T_0 |r|^2 + \kappa T_0 |t|^2 + \kappa T_p |a|^2, \qquad (5)$$

where T_0 is the temperature of the waveguide components, T_p is the plasma temperature, and κ is the Boltzmann constant. The quantities $|r|^2$, $|t|^2$, and $|a|^2$ are the power reflection, transmission, and absorption coefficients of the junction created by the presence of the plasma in the waveguide circuit. Power conservation requires $|r|^2 + |t|^2 + |a|^2 = 1$. Thus, the expression for the noise emission becomes

$$P_N = \kappa T_0 + \kappa(T_p - T_0) |a|^2. \qquad (6)$$

Note that in this configuration the presence of the plasma is detected by the receiver only when $T_p \neq T_0$ and $|a|^2 \neq 0$. Since we are interested only in the relative noise emission, we need know only the properties of the absorption coefficient

$$|a|^2 = \frac{4Z_0 \,\mathrm{Re}\,(Z')}{|2Z' + Z_0|^2}. \qquad (7)$$

Using the same values of parameters assumed in the reflection calculation, $|a|^2$ was computed as a function of (ω_c/ω), resulting in the curves of Fig. 11. The upper hybrid resonance emission effects are clearly present. There is no peak in emission at cyclotron resonance, in agreement with experiment. This results because Re $(Z_p) = 0$ at $(\omega_c/\omega) = 1$.

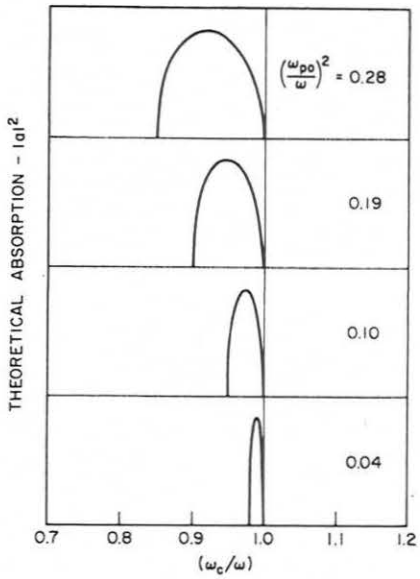

FIG. 11. Theoretical absorption ($|a|^2 \propto$ noise emission) vs magnetic field with electron density as a parameter.

V. DISCUSSION

The general simplicity and systematic form of the reflection and noise emission data are striking. The

[22] J. L. Lawson and G. E. Uhlenbeck, Eds., *Threshold Signals* (McGraw-Hill Book Company, New York, 1950), Chap. 4, p. 64.

reflection data show both cyclotron resonance and what have been interpreted as upper hybrid resonance effects. The emission data show only the upper hybrid resonance. Furthermore, the reflection and emission data for a given gas show an interesting correlation (recall the helium data, particularly). The simple cold plasma theory fails to predict the actual positions of the hybrid peaks. One would initially suspect the one-dimensional nature of the model as the source of the discrepancy. In fact, calculations[23] of the scattering and absorption of a plane wave by an infinite, but nonuniform cold plasma cylinder do show the hybrid peak rounded and shifted to a position between cyclotron resonance and maximum upper hybrid resonance. In this particular calculation the electrostatic approximation for the fields inside the plasma was *not* made. However, this calculation does not yield a cyclotron resonance peak either in scattering or absorption (emission). Only the upper hybrid resonances are important. Furthermore, no break in slope at cyclotron resonance (recall the argon emission data) is found in this calculation. Other calculations of absorption by cold plasmas of various geometries show only upper hybrid resonance effects.[18,24] Kuckes and Wong[25] have presented a calculation of the absorption in a one-dimensional inhomogeneous cold plasma which shows one peak at cyclotron resonance and one at the cutoff frequency which is the solution of $(\omega_c/\omega) + (\omega_p/\omega)^2 = 1$. However, their calculation was made with parameters appropriate to their experiments which were considerably different from ours. In particular, their experiments were performed with (ka) large ($\approx$10) while (ka) is small ($\approx$0.4) in our experiments, where a is the plasma radius. The more realistic calculation in cylindrical geometry[23] does not show these effects when ka is small. Tetenbaum and Bailey[7] have found evidence of the peaks of Kuckes and Wong in noise emission experiments. However, their measurements were carried out in a stimulated hot afterglow, and again in a geometry such that ka is large. When ka is large, multiple wave resonances and high-order multipole scattering terms become important. The absence of a cyclotron resonance peak in absorption thus appears to be an inherent property of the cold plasmas of the type considered here.

Of course, cold-plasma models are only approximate in the final analysis. The theory of electrostatic oscillations in inhomogeneous, hot plasmas yields standing wave normal modes whose oscillation frequencies are intimately related to the nonuniform electron density profile and the associated upper hybrid frequencies.[4,26] As is the case with the cold plasma modes, the hot-plasma modes are distributed in the band $[\omega_c, \omega_{h0}]$. At low temperatures and densities like those of our experiments, these modes are very closely spaced, approaching a continuum. Thus, the frequency domain distribution of modes for the hot and cold plasmas are very similar. However, examination of the general properties of these modes shows that one would expect a very high number of modes per given frequency range in the vicinity of cyclotron resonance. For our one-dimensional, cold-plasma model the presence of the transmission line is essential and produces the reflection peak at cyclotron resonance. Since the cylindrical scattering calculation[23] does not show this resonance, the role of the transmission line appears to be crucial. However, one might suspect that, in general, the cyclotron resonance effects observed (reflection peak and break in slope for emission) have some relation to this high density of modes.

Pulse-stimulated ringing experiments[11,27] in similar afterglow plasmas have shown that the long-time response is strongest at the frequencies ω_c and ω_{h0}. These results are qualitatively consistent with the cw data presented here. That is, from the cw data one would expect pulse measurements to show a double peak in the frequency domain. In fact, we have carried out pulse reflection and low-density ringing experiments which exhibit the same general behavior.[10,28] However, there is some question as to whether the pulse ringing occurs exactly at ω_{h0} or at some mean hybrid frequency as one would expect on the basis of our cw data. At very low electron densities such as those used in some of the ringing experiments, it is difficult to distinguish such differences quantitatively. One further fact supporting the upper hybrid resonance interpretation of the data is the existence of echoes observed in experiments with these same plasmas.[10] An inhomogeneous cold plasma theory successfully predicts some of the salient features of these echoes which are thought to involve directly upper hybrid plasma oscillations.

The importance of the nonuniform density profile

[23] R. W. Gould and R. H. Ault, Bull. Am. Phys. Soc. **13**, 888 (1968).
[24] J. L. Hirshfield and S. C. Brown, Phys. Rev. **122**, 719 (1961).
[25] A. F. Kuckes and A. Y. Wong, Phys. Fluids **8**, 1161 (1965).
[26] G. A. Pearson, Phys. Fluids **9**, 2454 (1966); H. L. Frisch and G. A. Pearson, *ibid.* **9**, 2464 (1966).
[27] D. E. Baldwin, D. M. Henderson, and J. L. Hirshfield, Phys. Rev. Letters **20**, 314 (1968).
[28] L. O. Bauer, Ph. D. thesis, California Institute of Technology (1968).

is clear. This profile gives the distribution of normal modes responsible for the breadth of the hybrid resonance peak in the data. Furthermore, this distribution of mode frequencies is essential to the echo processes observed in these same plasmas.[10] The difference between the data for helium and the other gases may result from a difference in the equilibrium density profiles. Having a quantitative theory one might be able to use the data to obtain information concerning plasma density profiles for various gases.

Finally, some remarks concerning the effect of geometry on calculated resonance frequencies are appropriate. For the one-dimensional electrostatic problems the hybrid frequencies $\omega_h^2 = \omega_c^2 + \omega_p^2$ are the relevant ones. In two-dimensional geometry numerical factors may be introduced, yielding modified hybrid frequencies. For example, a uniform cold-plasma cylinder exhibits a dipole resonance[29] at the frequency ω which is a solution of $\omega_p^2 = 2\omega(\omega - \omega_c)$. For low electron densities this formula gives a condition identical with the upper hybrid formula. However, at high electron densities, the two formulas differ quantitatively. Our experiments and interpretation do not exclude the presence of such numerical factors. However, none of the qualitative features of the phenomena are affected.

ACKNOWLEDGMENTS

We are indebted to R. S. Harp for comments and suggestions during the course of this research.

This work was supported by the United States Office of Naval Research under Contract Nonr 220(50). One of the authors (F.A.B) received support as a Howard Hughes Predoctoral Fellow and another of the authors (L.O.B.) received partial support from the Swiss Council of Scientific Research.

APPENDIX. CALCULATION OF THE COLD-PLASMA IMPEDANCE

We wish to evaluate the plasma impedance given in Eq. (3) for the parabolic density profile such that $\omega_p^2 = \omega_{p0}^2(1 - x^2/a^2)$. The basic problem is to compute the integral

$$I = \int_0^a \frac{dx}{(\omega_c^2 + \omega_{p0}^2 - \omega^2) - \omega_{p0}^2 x^2/a^2} \qquad \text{(A1)}$$

particularly when ω is in the range of upper hybrid frequencies $[\omega_c, \omega_{h0}]$. Expanding the integrand in Eq. (A1) in partial fractions yields

$$I = \frac{a^2}{2\omega_{p0}^2 b}\left(\int_0^a \frac{dx}{b - x} + \int_0^a \frac{dx}{b + x}\right), \qquad \text{(A2)}$$

where $b^2 = a^2(\omega_{h0}^2 - \omega^2)/(\omega_{p0}^2)$. The problem with the terms of Eq. (2) is that there is some value of x equal to b in the range $[0, a]$ when ω is in the upper hybrid range. Then the integrand of the first term in Eq. (A2) has a simple pole at $x = b$. If one considers collision effects, b has a small positive imaginary part (when $\omega_c < \omega < \omega_{h0}$) which goes to zero as the collision frequency goes to zero. Taking this limit of zero collision frequency is the correct way to evaluate the integrals of Eq. (A2)

$$I = \frac{a^2}{2\omega_{p0}^2 b}\left(\lim_{\epsilon \to 0} \int_0^a \frac{dx}{b - x + i\epsilon} + \int_0^a \frac{dx}{b + x}\right). \qquad \text{(A3)}$$

Using the Dirac formulation of the first integral in Eq. (A3) gives

$$I = \frac{a^2}{2\omega_{p0}^2 b}\left(P\int_0^a \frac{dx}{b - x} - i\pi + \int_0^a \frac{dx}{b + x}\right), \qquad \text{(A4)}$$

where P indicates that the Cauchy principal value should be taken. The evaluation of I is now straightforward:

$$I = \frac{a^2}{2\omega_{p0}^2 b}\left[\log\left(\frac{a + b}{a - b}\right) - i\pi\right].$$

For ω outside the upper hybrid range, the expression for Z_p can be found using standard integral tables:

$$\omega \leq \omega_c, \qquad Z_p = \frac{a}{i\omega\epsilon_0 A}\frac{\omega_c^2 - \omega^2}{\omega_{p0}(\omega_{h0}^2 - \omega^2)^{1/2}} \cdot \log\left(\frac{(\omega_{h0}^2 - \omega^2)^{1/2} + \omega_{p0}}{(\omega_{h0}^2 - \omega^2)^{1/2} - \omega_{p0}}\right),$$

$$\omega_c \leq \omega \leq \omega_{h0}, \qquad Z_p = \frac{a}{i\omega\epsilon_0 A}\frac{\omega_c^2 - \omega^2}{\omega_{p0}(\omega_{h0}^2 - \omega^2)^{1/2}} \cdot\left[\log\left(\frac{\omega_{p0} + (\omega_{h0}^2 - \omega^2)^{1/2}}{\omega_{p0} - (\omega_{h0}^2 - \omega^2)^{1/2}}\right) - i\pi\right],$$

$$\omega > \omega_{h0}, \qquad Z_p = \frac{-2a}{i\omega\epsilon_0 A}\frac{\omega_c^2 - \omega^2}{\omega_{p0}(\omega^2 - \omega_{h0}^2)^{1/2}} \cdot\tan^{-1}\left(\frac{\omega_{p0}}{(\omega^2 - \omega_{h0}^2)^{1/2}}\right).$$

[29] F. W. Crawford, G. S. Kino, and A. B. Cannara, J. Appl. Phys. **34**, 3168 (1963).